Monthly Notices of the ROYAL ASTRONOMICAL SOCIETY

MNRAS **544,** 1992–1998 (2025) https://doi.org/10.1093/mnras/staf967
Advance Access publication 2025 June 25

The X-ray class of the Carrington flare

Hugh S. Hudson [1,2] Edward W. Cliver,[3] Hisashi Hayakawa,[4] Ciarán D. Beggan [5] Ellen Clarke,[5] Peter Gallagher [6] Chris Osborne [1★] and Graham Woan[1]

[1]*SUPA School of Physics and Astronomy, University of Glasgow, Glasgow G12 8QQ, UK*
[2]*Space Sciences Laboratory, University of California, Berkeley, CA 94720, USA*
[3]*National Solar Observatory, 3665 Discovery Drive, Boulder, CO 80303, USA*
[4]*Institute for Space-Earth Environmental Research, Nagoya University, Nagoya, Japan*
[5]*British Geological Survey, Research Avenue South, Edinburgh EH14 4AP, UK*
[6]*Astronomy & Astrophysics Section, DIAS Dunsink Observatory, Dublin Institute for Advanced Studies, Dublin D15 XR2R, Ireland*

Accepted 2025 June 8. Received 2025 May 30; in original form 2025 April 24

ABSTRACT

The geomagnetic 'solar flare effect' (SFE) results from excess ionization produced by solar X-ray and EUV radiation in the Earth's upper atmosphere. The simultaneous detection of an SFE at the time of the Carrington flare in 1859 allows us to calibrate this event on the (revised) modern GOES X-ray scale. For this purpose, we make a basic correlation analysis of SFEs recorded at 1-min averaging at a single geomagnetic observatory, the Hartland station, as the site closest to London and the two original observing stations (Kew and Greenwich). We find the equivalent GOES magnitude of the Carrington event to have been $X105^{+41,-24}$ based on a sample of 39 X-class flare events observable as SFEs, with the estimate limited by systematic errors in the interpretation of the modern data. This estimate agrees with estimates based on the visual observations of the flare. This suggests that the Carrington flare was not a 'superflare' in the sense that it required physics beyond that needed for ordinary flares.

Key words: Sun: corona – Sun: UV radiation – Sun: X-rays.

1 INTRODUCTION

The first reported optical observation of a flare (Carrington 1859) was accompanied by the earliest reported case of a 'solar flare effect' (SFE) (Stewart 1861). The SFE phenomenon (also termed the *'magnetic crochet'*) remains useful as a proxy for solar X-ray and Extreme Ultraviolet (EUV) emissions (Cliver & Svalgaard 2004; Clarke et al. 2010; Curto 2020). The Carrington event certainly was a powerful flare, and it has caught the public imagination as the embodiment of a 'superflare' (Schaefer, King & Deliyannis 2000, who set this arbitrarily at an event total energy threshold of 10^{33} erg), capable of causing great damage to human society (e.g. Cliver et al. 2022). Two recent discoveries have further piqued interest in superflares: the tree-ring events (Miyake et al. 2012) and the powerful stellar flares from apparently solar-type stars (Maehara et al. 2012). The radioisotope events discovered in ancient tree-rings and ice cores suggest occasional solar sources of energetic particles (Usoskin et al. 2023) greatly outstripping even a huge solar eruption such as that of the flare SOL1956-02-23 (Meyer, Parker & Simpson 1956; McCracken, Shea & Smart 2023; Hayakawa et al. 2024). This event had the greatest high-energy particle fluence recorded since such observations began in the early 1940s. The Carrington event (as a 'superflare') notionally lies between the family of eruptive solar flares, and perhaps the physically different historic events inferred from radioisotope records and stellar photometry.

The optical observations of the Carrington flare (Carrington 1859; Hodgson 1859) fortuitously occurred shortly after the installation of the first recording magnetometers at Kew and Greenwich in the vicinity of London, with independently developed instrumentation. Routine observations at Kew had only begun in 1858 (Stewart 1860). The occurrence and morphology of the SFE had been noted immediately by Stewart, but the deeper implications only became clear once systematic flare observations had begun and we had achieved some understanding of the ionosphere (Bartels 1937). The original SFE records from Kew and Greenwich have survived, and recently Beggan et al. (2024) have made the data from both sites available in digital form.[1] Our data reduction assumes the $\Delta B_{\rm hor} = -131 \pm 10$ nT, as taken from the Kew observations; this is significantly different from the commonly accepted value of -110 nT (Newton 1943, *et seq.*). In this paper, we use the new value and a statistical sample of modern events to estimate the Geostationary Operational Environmental Satellite (GOES) soft X-ray magnitude[2] of the Carrington event. Section 2 describes the data, both historical and modern, and Section 3 discusses how to extrapolate the observed correlations to make a best estimate for

★ E-mail: christopher.osborne@glasgow.ac.uk

[1]https://doi.org/10.5285/c03ec758-d74d-4267-97fe-1be409f4c366
[2]This work uses the recently revised GOES magnitudes (Machol et al. 2022; Hudson et al. 2024).

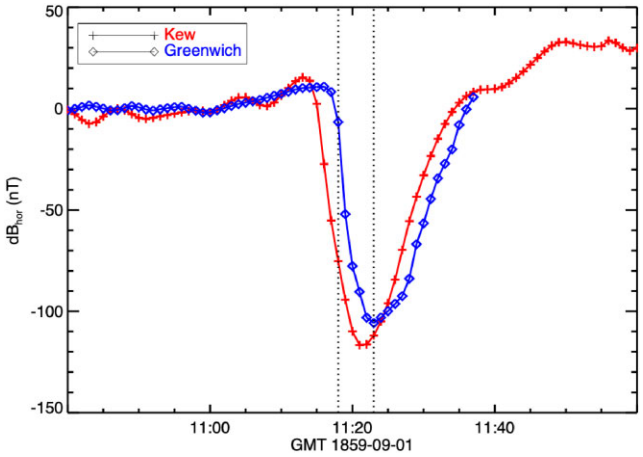

Figure 1. Digitized traces of the original paper recordings from the Kew and Greenwich magnetometers at the time of the Carrington event. The vertical dotted lines show Carrington's start and stop times for flare detection.

the X-ray magnitude. Generally, our analysis consists of a statistical survey of the 'slow' component of SFE response, as identified by Richmond & Venkateswaran (1971) with soft X-rays.

2 DATA

2.1 The Carrington event, 1859

The Beggan et al. (2024) digitization of the original geomagnetic records from the Kew and Greenwich observatories places the SFE magnitude at about −131 nT in the geomagnetic horizontal component $B_{\rm hor}$. Measurements of all three components of the field exist, but the $B_{\rm hor}$ variation usually provides the cleanest signature of an SFE and is the commonly adopted observable. The early recording systems consisted of rotating clockwork-driven drums to which photographically sensitive paper was fixed; light beams from the variometers wrote directly to this paper medium, which then needed chemical development to produce a permanent visible record. This type of recording produced detailed and permanent geomagnetic records, and it had only begun in 1858 (Stewart 1860) at Kew. This was just prior to the great solar activity in 1859 (Stewart 1861). The methods for calibration and characterization of this analogue system are imperfectly known, but fig. 1, from the Beggan et al. (2024) digitization, shows that the independent but similar instruments at Kew and Greenwich produced very comparable results. Indeed, the tight similarity of the two independent time series shows that the damping times were short enough to capture variations faster than a minute.

Fig. 1 also illustrates some of the problems with the metadata. The displacement of the two peak times from one another indicates some clock error. Carrington's flare observation began at 11:18 and ended at 11:23 Greenwich mean time, as indicated, and match reasonably well within our imperfect knowledge of the physical mechanisms involved; he estimated the precision of his time marks at 15 s (Carrington 1859). Note that the time on the Greenwich magnetogram has been revised and the time on the Kew magnetogram is only known via a handwritten start and end time. Finally, we can note the behaviour of the two magnetometer records just prior to the event. The Greenwich line appears to have greater smoothing, based on the small fluctuations in this interval. This suggests a somewhat longer damping time in its mechanism.

Table 1. Event List.

IAU identifier	Class[a]	$\Delta B_{\rm hor}$	Season
SOL1991-12-24T10:24	X2.00	−6.3	W
SOL1992-02-16T12:37	X2.10	−5.7	W
SOL1997-11-06T11:55	X13.2	−20.0	W
SOL1997-11-27T13:17	X3.80	−10.0	W
SOL1998-05-02T13:42	X1.60	11.7	S
SOL2000-06-06T13:39	X1.70	−11.0	S
SOL2000-07-11T13:10	X1.50	3.4	S
SOL2000-07-12T10:37	X3.00	2.0	S
SOL2000-07-14T10:24	X8.80	0.3	S
SOL2001-03-29T10:15	X2.70	0.5	S
SOL2001-04-02T10:14	X2.00	0.3	S
SOL2001-04-02T11:36	X1.50	−8.0	S
SOL2001-04-12T10:28	X3.00	9.4	S
SOL2001-04-15T13:50	X21.2	−40.0	S
SOL2001-09-24T10:38[b]	X3.70	−36.0	W
SOL2002-08-30T13:29	X2.20	9.2	S
SOL2003-03-18T12:08	X2.20	4.7	W
SOL2003-10-28T11:10	X25.8	−37.0	W
SOL2004-07-16T10:41	X1.60	−0.4	S
SOL2004-07-16T13:55	X5.50	−1.3	S
SOL2004-10-30T11:46	X1.80	−2.3	W
SOL2005-07-14T10:55[b]	X1.90	−4.0	S
SOL2006-12-05T10:35	X13.1	−10.0	W
SOL2011-09-22T11:01	X2.00	−5.4	W
SOL2013-11-19T10:26	X1.50	−4.5	W
SOL2014-06-10T11:42	X3.30	−3.8	S
SOL2014-06-10T12:52	X2.20	3.0	S
SOL2014-10-26T10:56	X2.80	−13.0	W
SOL2017-09-06T12:02	X14.8	−9.9	S
SOL2022-04-30T13:47	X1.10	−2.2	S
SOL2022-05-03T13:25	X1.10	−4.6	S
SOL2022-05-10T13:55	X1.50	−5.7	S
SOL2024-02-09T13:14	X3.30	−11.0	W
SOL2024-05-05T11:54	X1.20	0.6	S
SOL2024-05-11T11:44[b]	X1.50	167.0	S
SOL2024-05-14T16:51	X8.70	−4.1	S
SOL2024-06-10T11:08	X1.50	0.7	S
SOL2024-07-16T13:26	X1.90	3.3	S
SOL2024-08-05T13:40	X1.70	−1.6	S
SOL2024-10-03T12:18	X9.00	−23.0	W
SOL2024-11-06T13:40	X2.30	−0.8	W
SOL2025-01-03T11:39	X1.20	−6.5	W

Notes. [a]Revised classifications (Hudson et al. 2024).
[b]Discarded.

2.2 The Hartland SFE events, 1991–2025

The Hartland observatory (HAD) of the British Geological Survey is the intermagnet[3] site geographically closest[4] to the Kew and Greenwich observatories, the sites of the original geomagnetic observations (Stewart 1861). We have accordingly based our analysis on this site (HAD) as the best proxy. Since 1991 HAD reported observations during 42 X-class (original scale; see Hudson et al. 2024) flares, based on the current National Oceanic and Atmospheric Administration (NOAA) flare lists and restricting the soft X-ray peak times to the range 10:00–14:00 UT. Table 1 lists the selected events, with *Class* giving the peak GOES flux on the modern scale, background-subtracted as in Hudson et al. (2024), and *Season* W for winter, S for summer. We have chosen to use 1-min sampling

[3]https://intermagnet.org
[4]HAD 51.0N,4.5W; GRW 51.5N,0.0E; KEW 51.5N,0.3W.

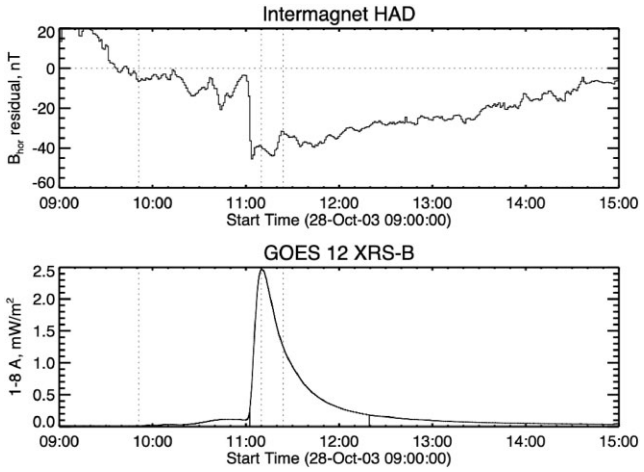

Figure 2. The most extreme flare of our sample, SOL2003-10-28 (X25.8 adjusted), which occurred during geomagnetically disturbed conditions but which none the less shows good coincidence with at least the initial development of the SFE. The dotted lines show the GOES times, and we note that NOAA's definition of end time is just at the 50 per cent peak level. The GOES data here are from 2-s sampling, but the reference times are based on 1-min data.

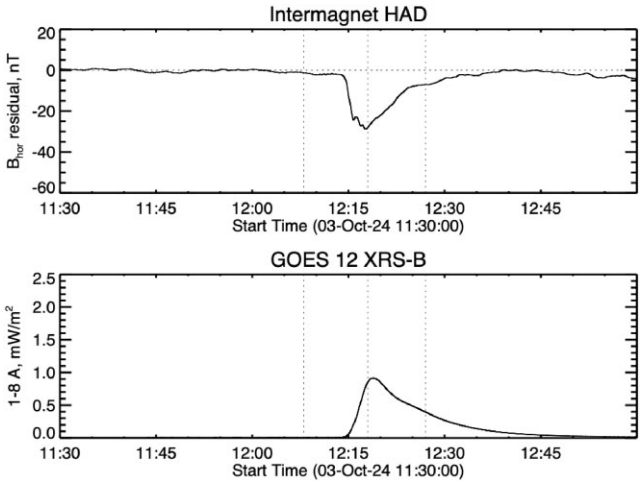

Figure 3. A more typical major event, SOL2024-10-03 (X9.0 adjusted), which occurred during less-disturbed geomagnetic conditions and actually resolves more of the SFE time structure with 1-s data cadence from the HAD observatory. Here, for uniformity, we use the GOES-16 1-min data. See the text for some further comments about this interesting event. These plots have the same scaling as Fig. 2, but on only a quarter of the time span.

for uniformity and have discarded three events because of high geomagnetic activity, as marked in the table.

This simplistic approach assumes that soft X-rays contribute strongly to SFE occurrence, even though many of the weaker GOES events in Table 1 did not produce events in the International Association of Geomagnetism and Aeronomy (IAGA) 'rapid events' data base[5] (Curto et al. 2023). Our analysis thus avoids the need for morphological classification and allows non-detections to be integrated statistically, based on their estimated uncertainties. Our model explictly ignores the known importance of EUV contributions to SFE (e.g. Curto et al. 1994) since reliable data bases have only recently begun; this is a recognized limitation contributing variance to our estimation.

Fig. 2 shows an exceptional case of this correlation; the well-known event SOL2003-10-28 (X25.8 new scale) was the most energetic one in our sample and occurred during geomagnetically disturbed conditions. We also show a more typical major event (SOL2024-10-03) in Fig. 3. This is on the same amplitude scale as in Fig. 2 but for a briefer time interval. Here, the geomagnetic background fluctuations are much smaller. Fig. 4, based on 1-s geomagnetic data, illustrates how geomagnetic variability interferes with the SFE estimations across all time-scales, showing three consecutive days of HAD records. For this event our algorithm (pre-flare variability over 10 min) found an uncertainty estimation of only 1.2 nT, missing the significant variance on longer time-scales.

We note also that the event in Fig. 3 has some interesting properties. One can see the flare's QPP (quasi-periodic pulsations, as described for this event by Li 2025) as wiggles near the peak of the SFE signal, indicating an effective recombination time for the excess ionization that must be no longer than the major pulsation period of some tens of seconds; see also O'Hare et al. (2025) in this context.

In the analysis, we have used the assumption of an approximate time correlation between an SFE and the related GOES soft X-ray burst in the following ways: we define a (geomagnetic) background interval as the 10-min period just prior to the listed GOES start time,

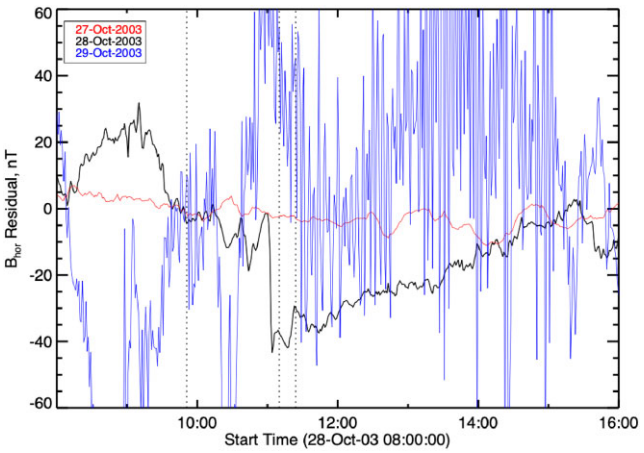

Figure 4. This figure gives a more detailed view of the SOL2003-10-28 event, using 1-s HAD geomagnetic records for this event (X25.8 adjusted). It shows 3 d of geomagnetic data, during which the geomagnetic storm on October 29 would have obscured even this major event.

and ΔB_h as the minimum of B_h (1-min sampling) during the interval between the listed GOES maximum and end times. We also estimate an uncertainty for each ΔB_h as the standard deviation of the 10-point pre-flare sample. This captures some of the unpredictable variance of the geomagnetic field in an approximate way but is reproducible and not subject to selection bias. The 10-min interval approximately matches the typical time-scale of an SFE. On the assumption of GOES correlation, we down-select from 42 to 39 events by requiring the SFE peak time to be within 6 min of the GOES maximum time and by rejecting events with extreme geomagnetic conditions. The well-studied 'Bastille Day' flare, SOL2000-07-14 (X8.8) in Table 1, appeared at the right time for HAD, but with extremely disturbed geomagnetic conditions.

[5]https://www.obsebre.es/en/variations/rapid

Table 2. Data fits, $\Delta B_{\rm hor} = A + BX$, Summer/Winter.

Data	N	GOES X1[a]	$-\Delta B_h$ nT	A nT	B nT/X[b]
S	24	3.97	3.56	$+1.59 \pm 0.100$	-1.63 ± 0.018
W	15	5.74	7.89	-5.30 ± 0.089	-0.86 ± 0.014
All	39	4.65	6.22	-2.24 ± 0.067	-1.22 ± 0.011

Notes. [a] Mean values of corrected GOES class.
[b] $Xn = n \times 10^{-4}$ W/m^2.

3 EXTRAPOLATION

We seek to extrapolate from the modern data base of SFEs to the magnitude of the Carrington SFE. In addition to the uncertainties in measurement, usually of order 0.4 nT for an INTERMAGNET observatory (e.g. Lesur et al. 2017), we have the problem of a small sample size (only 10 events for which $\Delta B_{\rm hor} < -10$ nT). The SFE process overall has many uncertainties in terms of ionospheric/magnetospheric electrodynamics, atmospheric chemistry and wind patterns, and local geology. In addition a simple linear extrapolation may not be correct in any case, since SFE current magnitudes for major events can exceed those of the background quiet-time diurnal variation (henceforth Sq, e.g. Curto 2020). Nevertheless all of the events have signals consistent with a negative $\Delta B_{\rm hor}$. In all of our estimates here, we assume linearity and also simultaneity with the GOES 1–8 Å flare. In the following, we describe in detail our approach to establishing the estimation and its uncertainties.

The cleanly observed event SOL2024-10-03 (Fig. 3) by itself would suggest a proportional factor of about -2.5 nT/Xn for this X9 event, scaling the Carrington event to ∼X52 based on the Carrington SFE at $\Delta B_{\rm hor} = -131 \pm 10$ nT, with only small measurement errors. Taking the means for the 39/42 selected events gives the result $\Delta B/Xn \approx -1.34$ nT/Xn, as shown in Table 2, putting the Carrington magnitude at X98. These two estimates do not agree within error uncertainties, consistent with the presence of other factors affecting the variance in our sample.

We made weighted two-parameter linear fits (Table 2) to the correlation between GOES peak flux and SFE magnitude for the 39 valid events, as shown in Fig. 5. The uncertainties of the geomagnetic measurements come mainly from various forms of dynamic activity in the ionosphere and the magnetosphere, and these can have broadband and unpredictable variability over and above the regular Sq diurnal variation (Graham 1724; Svalgaard 2016; Yamazaki & Maute 2017). We have chosen to estimate the magnitude of the flare-time geomagnetic fluctuations by taking the 10 min prior to the NOAA start time for each flare, and using its variance as a proxy. Over the 39 selected events, this estimate had a mean of 2.4 nT but a median of only 1.0 nT, reflecting the presence of increased but unavoidable geomagnetic activity on some of the flare days. These variations should have no direct correlation with the SFE physics itself, and so we use them but weight the flare values accordingly.

3.1 Ensemble results

The results in Fig. 5 confirm the roughly linear dependence of SFE magnitude with soft X-ray flux (Sastri & Murthy 1975). For our 39-event sample, we calculate a Pearson correlation coefficient for unweighted data of $\rho = -0.36$ (0.027), roughly a 95 per cent confidence level. The figure shows the uncertainties of the individual measurements at $\pm 3\sigma$, frequently smaller than the symbol size in the graphic. The scatter relative to the linear fit therefore reflects strong systematic uncertainties that could come from any number

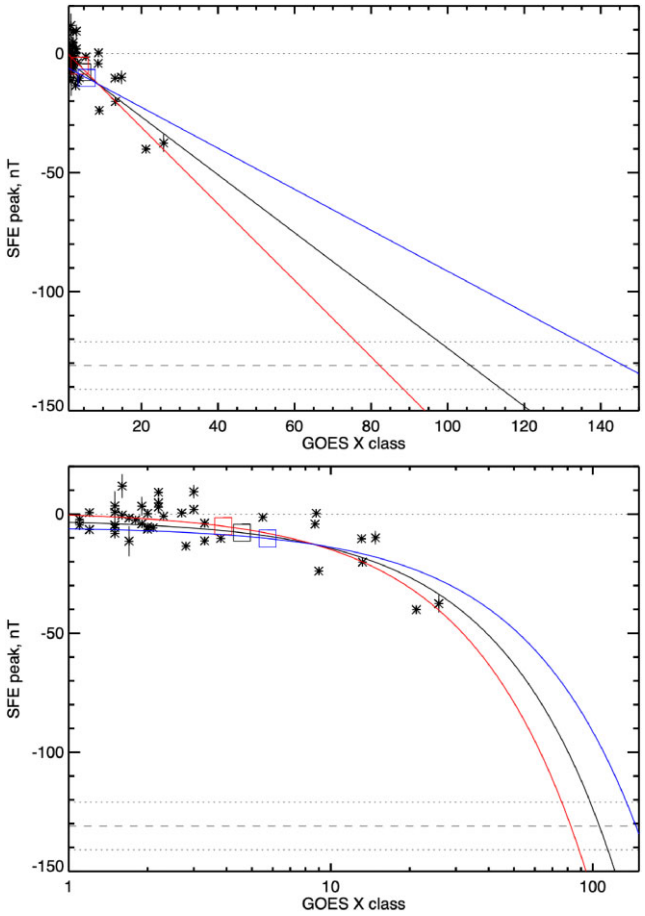

Figure 5. Linear fits to the correlation between GOES peak flux and SFE magnitude. The dashed line at bottom shows the SFE magnitude for the Carrington event (Beggan et al. 2024) at $\Delta B_{\rm hor} = -131$ nT, with dotted lines at ± 10 nT. The black fit line refers to the full data set (shown as points with errors, mostly smaller than the symbol widths; the blue (upper) and red (lower) lines are for fits to the Winter and Summer subsets, repectively. The lower panel shows the same linear fits but with log scaling on the X-axis. The square boxes show the mean values.

of effects. As listed in Table 1, we have divided the events by the latitude of the subsolar point: Winter (15 events) and Summer (24 events), noting that the Carrington event itself occurred in summer, but less than a month from the equinox. For this sample the fits are strikingly different, though in each case with only small formal errors. The best fit for all 39 events without selection predicts a Carrington magnitude of X105±2 based upon formal errors, assuming a two-parameter weighted fit to the linear function $B_{\rm hor} = A + BX$. This precision has no relevance to our final result owing to the presence of uncontrolled systematic errors, but it does suggest that a more sophisticated statistical survey can do better.

The data in Fig. 5 show considerable scatter, well in excess of the formal errors. This scatter also appears in the zenith-angle (Z) dependence of the SFE magnitudes (Fig. 6). For our 39-event sample, we find the linear fit $\Delta B_{\rm hor} = 2.35 \pm 0.18 - (0.156 \pm 0.003)Z$ nT, formally significant but with the correlation heavily confused by systematic errors. The mean values are $[\overline{Z}, \overline{\Delta B_{\rm hor}}] = [50.6^\circ, -6.22 \pm 0.05$ nT]. Note that our time window of ±2 h permitted zenith angles as great as 76°.

Based on the presence of this large scatter, we resort to a basic subdivision of the data set into two roughly equal parts, and have chosen a

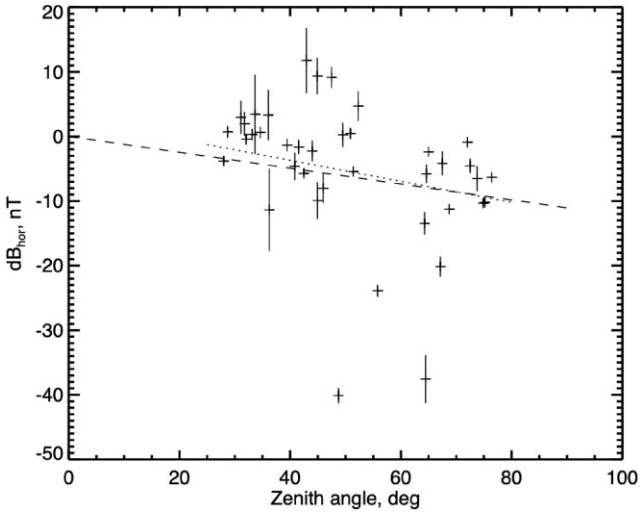

Figure 6. Zenith-angle dependence (see the text for fit values). Note that the error flags are 3σ for clarity. The dotted line shows the two-parameter linear fit (see the text), and the dashed line the simple proportional scaling.

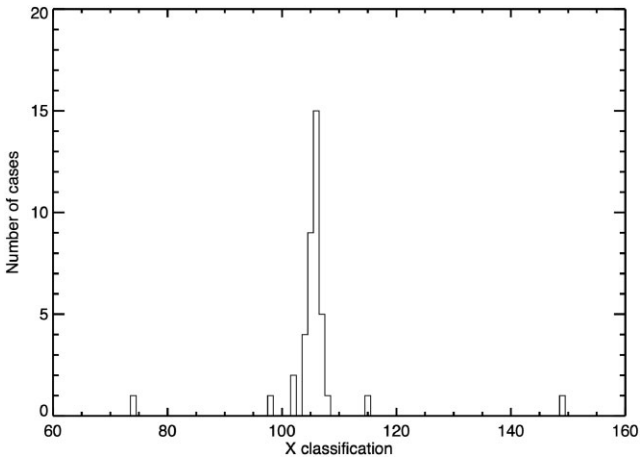

Figure 7. Histogram of predicted Carrington X-class from groups of 38 SFEs, omitting each of the 39 selected events one by one.

summer/winter separation for this purpose. Any such subdivision can illustrate the effects of other known and unknown sources of variance in the complicated chain of processes involved in producing an SFE (e.g. Richmond & Venkateswaran 1971; Richmond 2019). Direct corrections for some of these effects could be sought, but might not eliminate much of the variance. These would include effects such as the dependence on zenith angle, Sq vortex centre location, EUV or X-ray spectral variations, upper-atmospheric tides and winds, etc. Our sample of 39 events, using HAD only to match the 1859 geomagnetic observations as closely as possible, thus suffers from small-number statistics, in the sense that the data are too few to subdivide in efforts to correlate with possibly sources of systematic error.

3.2 Uncertainties

We exhibit the effects of small-number statistics via Fig. 7, which shows the histogram of the predicted class of the Carrington event for sets of 38 flares, omitting each individual SFE in turn and thereby examining its effect on the ensemble analysis.

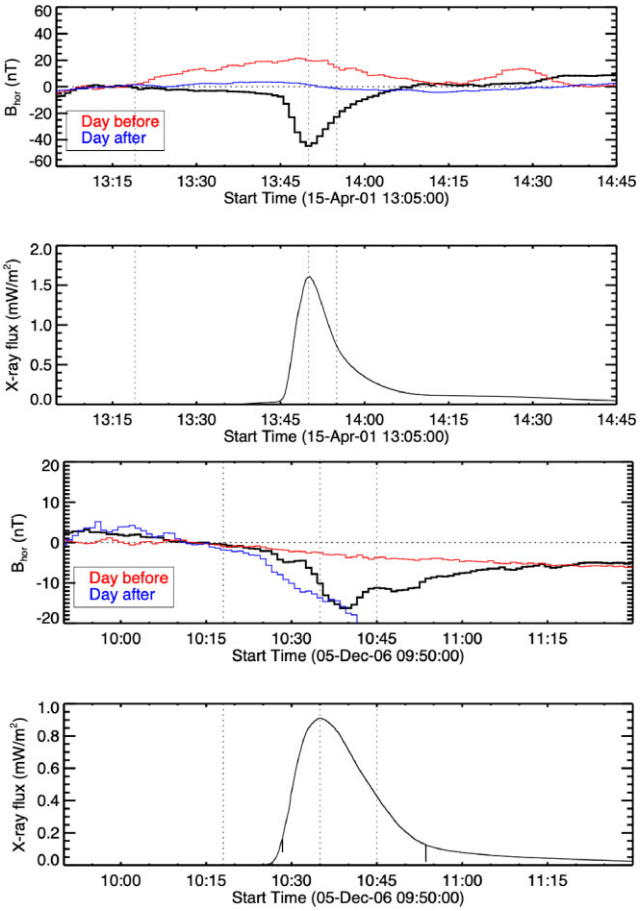

Figure 8. Comparison of the geomagnetic and X-ray data for the two exceptional events. The red and blue geomagnetic data are from the day before the event and the day after the event, with all three curves normalized to a pre-GOES start time interval. The X-ray data are the standard GOES 1–8 Å band on a linear scale.

We can clearly identify the preferred extrapolation result of about X105 from Fig. 5, but we can also see two specific flares (identified as SOL2001-04-15 and SOL2006-12-05) as the extreme outliers at the high and low values, respectively. These individual well-observed events each grossly alter the extrapolation result and together suggest the broad range X74–X149, comparable to the X81-X146 result from the ensemble analysis. Fig. 8 shows these events in detail, including comparisons with previous and following days to help understand the background geomagnetic variability. Our algorithm for error estimation, based on 10-min samples just prior to the GOES start time, can only reflect rapid variability on this time-scale, and slower variations will be ignored. This uncertainty clearly shows up in the upper panel (SOL2001-04-15), where the day-before diurnal pattern differs by almost 20 nT from that of the following day. The Potsdam Kp-index values (Matzka et al. 2021) were $[3^+, 4^+, 2^-]$ on these 3 d. For SOL2005-12-06 we find $[4^+, 3^-, 2]$, so for both of these anomalous events we note moderately disturbed geomagnetic conditions.

The conclusion from this exercise is that the two anomalous events may have larger uncertainties than our algorithm estimates, but in fact this does not matter, since the fits actually omit the questionable events in each case. At this level of analysis, we must make the conservative conclusion and accept the large variance they add to our 39-event sample. The final Carrington event classification

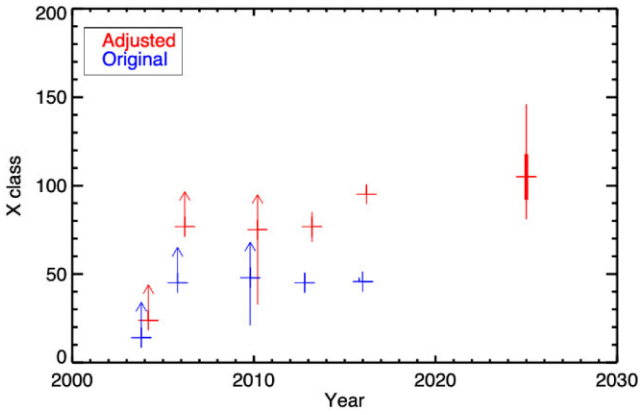

Figure 9. Estimates of the Carrington flare's X-ray magnitude, in GOES X-class units, as listed in Table 3, with the present result shown with formal errors as well as best estimates. The earlier estimates are in blue as published. The red points show the same after adjustment for the new GOES classification scale, and to the Beggan et al. (2024) estimate of the Carrington SFE magnitude.

therefore comes from the event subsets shown in Fig. 5, which is $X105^{+41,-24}$. The formal errors are smaller, roughly comparable with those adopted for the Carrington-event data in Fig. 1 (approximately 10 nT, corresponding to about 7 X units), as reported by Beggan et al. (2024).

4 IMPLICATIONS FOR THE CARRINGTON EVENT

The two relevant records from the time of the original Carrington observations are those of Carrington (1859) and Hodgson (1859), which describe the visual appearance of the flare, and the geomagnetic recordings we have studied here. Recently Hayakawa et al. (2023) have revisited the visual data, relating them to the GOES flare scale via scalings based on total flare energy to obtain a GOES class estimate of $X80^{+46,-34}$. The magnetic and visual estimates thus agree within uncertainties. Our new SFE-based results roughly double the estimated X class of the Carrington event, as based on earlier similar estimates, and are a factor of six above the conservative lower limit of X17 (corrected) originally set by Cliver & Svalgaard (2004) (Fig. 9). Table 3 lists the estimates with linear adjustments for GOES scaling and with the uniform assumption of $\Delta B_{\rm hor} = -131$ nT. This is only a rough approximation for the physics of the Curto, Castell & Del Moral (2016) model, but it places the various estimates on an even footing based on the basic extensive parameters.

The event magnitude X105 needs to be placed in the context of the occurrence distribution function of major flares. As compiled by Hudson et al. (2024) for GOES events in the 1975–2024 time range, this distribution follows a clean power law up to about X10, and then steepens significantly. This means that fewer extremely powerful events should be expected, as compared with the numbers estimated from simple extension of the power law. The expected return time of about 500 yr is roughly consistent with the age of the Carrington event. Using extreme-value theory Elvidge & Angling (2018) suggest a range X43–X129 (modern scale) for 150-yr return magnitude, and using an empirical distribution suggested by Sakurai (2022), Hudson et al. (2024) give X60–X115 for a 100-yr return magnitude. Our result fits within these broad ranges.

The large uncertainties in the predicted event magnitude reflect our ignorance of the environmental parameters for individual events, as well as the SFE physics itself, and also reflect the small size of the data sample. Because we restricted our study to the single magnetic observatory (HAD) closest to Kew and Greenwhich, a future study could greatly increase the data available – by extending the local-time range alone, by a factor of about six. Within a larger data set, it should be possible to discover correlations that could help to improve the prediction. On the solar side, this work has explicitly assumed that soft X-rays produce SFEs, but the spectral distribution of the X-rays was not considered. We also now have much-improved Lyman-alpha measurements, and a future statistical study could make a much more detailed prescription of the actual SFE causation. We note that Curto et al. (2016) have already incorporated EUV data in a detailed model comparing the Carrington event with the 'Halloween' event SOL2003-11-04, including an estimate of return time consistent with our statistical results.

Table 3. SFE-based estimates[a].

Reference	Original (Xn)	Adjusted (Xn)
Cliver & Svalgaard (2004)	> 10	> 17
Boteler (2006)	45	77
Clarke et al. (2010)	$> 48^{-27}$	$> 75^{-42}$
Cliver & Dietrich (2013)[b]	$45^{+5,-5}$	$77^{+9,-9}$
Curto et al. (2016)[b]	$46^{+2,-2}$	$95^{+5,-5}$
This work (2025)		$105^{+41,-24}$

Notes. [a]Adjusted to the modern GOES scale and to a Carrington event magnitude $\Delta B_{\rm hor} = -131$ nT.
[b]Our adjustment to this result is a simple linear approximation.

5 CONCLUSION

In this article, we have described a simple re-interpretation of the X-ray magnitude of the Carrington flare. We have used a modern-era set of 39 X-class flares observed at the Hartland geomagnetic observatory, the closest site to London (Kew and Greenwich). With the assumption that SFEs have a strong association with GOES soft X-rays, we have found an (anti)correlation between the GOES 1–8 Å peak flux and the SFE magnitude $\Delta B_{\rm hor}$. Based on a recent digitization and study of the permanent records from the original Kew observations, which assign an SFE magnitude for the Carrington event to be $\Delta B_{\rm hor} = -131 \pm 10$ nT, we have extrapolated to find a Carrington flare soft X-ray magnitude of $X105^{+41,-24}$, as limited by systematic errors in the modern data. This result is broadly consistent with independent estimates from visual records, $X80^{+46,-X34}$ (Hayakawa et al. 2023) and with earlier estimates based on the Carrington SFE. Better control of uncertainties should be possible in the future and would lead to a more exact result, but we can already recognize that the Carrington flare does not deserve the name 'superflare' in the sense that its occurrence matches the expectation from the best possible characterization of the occurrence distribution function of GOES X-ray fluxes.

ACKNOWLEDGEMENTS

We thank the referee for detailed commentary. The results presented in this paper rely on data collected at magnetic observatories. We thank the national institutes that support them and INTERMAGNET for promoting high standards of magnetic observatory practice (www.intermagnet.org). We especially thank the contemporaneous observers at Kew and Greenwich for having industriously operated these valuable magnetic measurements. HSH thanks the University of Glasgow for hospitality and for re-introducing him to geomagnetic

measurements. HH thanks financial supports of JSPS Grants-in-Aid JP25K17436, the ISEE director's leadership fund for FYs 2021–2025, Tokai Pathways to Global Excellence (Nagoya University) of the Strategic Professional Development Program for Young Researchers (MEXT), and the young researcher units for the advancement of new and undeveloped fields, Institute for Advanced Research, Nagoya University of the Program for Promoting the Enhancement of Research Universities. He also thanks Ebro University for providing their SFE data base (Curto et al. 2023). CMO is grateful to the Royal Astronomical Society's Norman Lockyer fellowship, and the University of Glasgow's Lord Kelvin/Adam Smith Leadership fellowship for financially supporting this work.

DATA AVAILABILITY

The data underlying this article are available at https://intermagnet.org and https://www.ncei.noaa.gov for geomagnetic and solar X-ray records, respectively.

REFERENCES

Bartels J., 1937, Terr. Magn. Atmos. Elect., 42, 235
Beggan C. D., Clarke E., Lawrence E., Eaton E., Williamson J., Matsumoto K., Hayakawa H., 2024, Space Weather, 22, e2023SW003807
Boteler D. H., 2006, Adv. Space Res., 38, 301
Carrington R. C., 1859, MNRAS, 20, 13
Clarke E., Rodger C., Clilverd M., Humphries T., Baillie O., Thomson A., 2010, National Astronomy Meeting (NAM), UK
Cliver E. W., Dietrich W. F., 2013, J. Space Weather Space Clim., 3, A260000
Cliver E. W., Svalgaard L., 2004, Sol. Phys., 224, 407
Cliver E. W., Schrijver C. J., Shibata K., Usoskin I. G., 2022, Living Rev. Sol. Phys., 19, 2
Curto J. J., 2020, J. Space Weather Space Clim., 10, 27
Curto J. J., Amory-Mazaudier C., Torta J. M., Menvielle M., 1994, J. Geophys. Res., 99, 23289
Curto J. J., Castell J., Del Moral F., 2016, J. Space Weather Space Clim., 6, A23
Curto J. J., Segarra A., Altadill D., Chamboodut A., 2023, Geosci. Data J., 10, 99
Elvidge S., Angling M. J., 2018, Space Weather, 16, 417
Graham G., 1724, Philos. Trans. R. Soc. Lond. Ser. I, 33, 96
Hayakawa H., Bechet S., Clette F., Hudson H. S., Maehara H., Namekata K., Notsu Y., 2023, ApJ, 954, L3
Hayakawa H., Koldobskiy S., Mishev A., Poluianov S., Gil A., Usoskina I., Usoskin I., 2024, A&A, 684, A46
Hodgson R., 1859, MNRAS, 20, 15
Hudson H., Cliver E., White S., Machol J., Peck C., Tolbert K., Viereck R., Zarro D., 2024, Sol. Phys., 299, 39
Lesur V., Heumez B., Telali A., Lalanne X., Soloviev A., 2017, Ann. Geophys., 35, 939
Li D., 2025, A&A, 695, L4
McCracken K. G., Shea M. A., Smart D. F., 2023, Adv. Space Res., 72, 3414
Machol J., Viereck R., Peck C., Mothersbaugh III J., 2022, Technical Report, GOES XRS operational data (NOAA). Available at: https://www.ngdc.noaa.gov/stp/satellite/goes/doc/GOES_XRS_readme.pdf
Maehara H. et al., 2012, Nature, 485, 478
Matzka J., Stolle C., Yamazaki Y., Bronkalla O., Morschhauser A., 2021, Space Weather, 19, e2020SW002641
Meyer P., Parker E. N., Simpson J. A., 1956, Phys. Rev., 104, 768
Miyake F., Nagaya K., Masuda K., Nakamura T., 2012, Nature, 486, 240
Newton H. W., 1943, MNRAS, 103, 244
O'Hare A. N., Bekker S., Hayes L. A., Milligan R. O., 2025, J. Geophys. Res. Space. Phys., 130, e2024JA033493
Richmond A. D., 2019, J. Geophys. Res. Space Phys., 124, 9154
Richmond A. D., Venkateswaran S. V., 1971, Radio Sci., 6, 139
Sakurai T., 2022, Physics, 5, 11
Sastri J. H., Murthy B. S., 1975, Sol. Phys., 41, 477
Schaefer B. E., King J. R., Deliyannis C. P., 2000, ApJ, 529, 1026
Stewart B., 1860, Rep. Br. Ass. Advmt. Sci., 30, xxxi
Stewart B., 1861, Philos. Trans. R. Soc. Lond. Ser. I, 151, 423
Svalgaard L., 2016, Sol. Phys., 291, 2981
Usoskin I. et al., 2023, Space Sci. Rev., 219, 73
Yamazaki Y., Maute A., 2017, Space Sci. Rev., 206, 299

This paper has been typeset from a TEX/LATEX file prepared by the author.